Communication

Exploring the Combined Action of Adding Pertuzumab to the Branded Trastuzumab versus Trastuzumab Biosimilars for Treating HER2+ Breast Cancer

Emma Franco-Mateos , Virginia Souza-Egipsy , Laura García-Estévez , Jose Manuel Perez-García , Maria Gion , Laia Garrigós , Patricia Cortez , Cristina Saavedra , Patricia Gómez , Carolina Ortiz , Victor L. Cruz , Javier Ramos , Javier Cortés , Juan F. Vega *

Posted Date: 26 February 2024

doi: 10.20944/preprints202402.1423.v1

Keywords: HER2+ breast cancer, monoclonal antibodies, trastuzumab biosimilars.

Communication

Exploring the Combined Action of Adding Pertuzumab to the Branded Trastuzumab versus Trastuzumab Biosimilars for Treating HER2+ Breast Cancer

Emma Franco-Mateos [1], Virginia Souza-Egipsy [1], Laura García-Estévez [2], José Pérez-García [3,4,5], María Gion [6], Laia Garrigós [3], Patricia Cortez [7], Cristina Saavedra [6], Patricia Gómez [3], Carolina Ortiz [3], Víctor L. Cruz [1], Javier Ramos [1], Javier Cortés [3,4,8,†] and Juan F. Vega [1,*]

[1] BIOPHYM, Department of Macromolecular Physics, Instituto de Estructura de la Materia, IEM-CSIC, C/Serrano 113 bis, 28006 Madrid, Spain
[2] Breast Cancer Department, MD Anderson Cancer Center, Madrid, Spain
[3] International Breast Cancer Center (IBCC), Pangaea Oncology, Quiron Hospital, Barcelona, Spain
[4] Medica Scientia Innovation Research (MedSIR), Barcelona, Spain
[5] Medica Scientia Innovation Research (MedSIR), Ridgewood, New Jersey
[6] Medical Oncology Department, Ramón y Cajal University Hospital, Madrid, Spain
[7] IOB, Institute of Oncology, Madrid, Spain
[8] Faculty of Biomedical and Health Sciences, Department of Medicine, Universidad Europea de Madrid, Madrid, Spain
* Correspondence: jf.vega@csic.es
† J.C. was at Vall d'Hebron Institute of Oncology, Barcelona, Spain, during the development of this work.

Abstract: The binding activity of various trastuzumab biosimilars versus the branded trastuzumab towards the glycosylated extracellular domain of the HER2 target in the presence of pertuzumab was investigated. We employed size exclusion chromatography with tetra-detection methodology to simultaneously determine absolute molecular weight, concentration, molecular size, and intrinsic viscosity. All trastuzumab molecules in solution exhibit analogous behavior in their binary action towards HER2 regardless of the order of addition of trastuzumab/pertuzumab. This analogous behavior of all trastuzumab molecules, including biosimilars, highlights the robustness and consistency of their binding activity towards HER2. Furthermore, the addition of HER2 to a mixture of trastuzumab and pertuzumab leads to increased formation of high-order HER2 complexes, up to concentrations of one order of magnitude higher than in the case of sequential addition. The observed increase suggests a potential synergistic effect between these antibodies, which could enhance their therapeutic efficacy in HER2-positive cancers. These findings underscore the importance of understanding the complex interplay between therapeutic antibodies and their target antigens, providing valuable insights for the development of more effective treatment strategies.

Keywords: HER2+ breast cancer; monoclonal antibodies; trastuzumab biosimilars

1. Introduction

Monoclonal antibodies (mAbs) have revolutionized cancer treatment over recent years, offering precise targeting to specific proteins or cells. In the case of breast cancer, several mAbs-based therapies have been developed and approved for use [1]. Notable among these are trastuzumab and pertuzumab, and more recently tucatinib and trastuzumab-deruxtecam [2]. These drugs target the very aggressive HER2-positive (HER2+) cancer cells by blocking the action of the HER2 protein [3,4]. Presently, 5-year survival rate is increasing up to 90 % in HER2+ early breast cancer treated with chemotherapy and combined or dual mAbs trastuzumab and pertuzumab therapies, as they show

 doi:10.20944/preprints202402.1423.v1

complementary mechanisms of action [5]. Clinical trials and meta-analyses have reported cases of sequential addition in patients undergoing dual anti-HER2 therapies. Jagosky and Liu [6,7] have recently reviewed several studies that support the substantial improvement in the outcome of HER2+ breast cancer patients with combined therapy of pertuzumab and trastuzumab [8–17]. Additionally, it has been demonstrated that the combination of trastuzumab emtansine (T-DM1) and pertuzumab exhibits synergistic cytotoxic activity in cell culture and enhanced antitumor activity [18]. Moreover, the results have indicated that the safety of dual-target therapy is similar to that of single-target therapy [11,19]. By the other hand, biosimilars highly resemble the branded drugs, but with the advantage of quicker development, lower cost of production and greater availability. As the development process of a biosimilar is somewhat different to that of the reference product, it is possible to include minor changes or additions to the protein structure that can produce a drug with different efficacy or side effect profiles. However, a biosimilar drug may not be an exact copy of the reference product, but it must maintain identical or even improve its mechanisms of action, dosage and route of administration, and effectiveness [20–22]. Several biosimilars of Herceptin® [Genentech, Inc.] have been approved for use in breast cancer treatment, including Ontruzant® [N.V. Organon] and Herzuma® [Celltrion, Inc.] [23]. In this study, we assessed the ability of each of these antibodies to bind to HER2 in the presence of the pertuzumab Perjeta® [Genentech, Inc.], and investigated the order of addition of the mAbs to HER2 in solution. Our findings could provide insights into potential combination therapies for HER2+ breast cancer and contribute to the optimization of treatment efficacy.

The chosen methodology for investigating the binding process was size exclusion chromatography with tetra-detection (SEC-TD) in solution. This analytical approach offers numerous advantages for examining protein-protein interactions or the binding between mAbs and target proteins. SEC-TD is fast, efficient, cost-effective, and sensitive, and it enables the simultaneous detection of proteins and complexes in a single analytical run. Furthermore, it has been reported that binding experiments in solution may offer more realistic results that, for example, protocols using antibody support techniques [24]. In this technique, biomacromolecules of varying sizes in the solution are separated in the column and eluted at distinct times. The eluent then passes through the tetra-detection system, which comprises four sequential detectors - ultraviolet (UV), light scattering (LS), refractive index (RI), and viscosimeter (VIS). This enables the measurement of the composition, absolute molecular weight and size, concentration, and molecular density or intrinsic viscosity of the biomacromolecules, thus providing a comprehensive overview of the protein-protein interactions and stability of the complexes formed [25–29].

2. Results and discussion

The hydrodynamic and electrostatic characterization results of the mAbs are presented in Figures S1-S3 and Tables S1 and S2 of the Supplementary Material archive. The findings depicted in Figures S1 to S3 indicate a considerable level of resemblance among the examined mAbs. Specifically, the diffusion coefficient (representing hydrodynamic size) exhibits variances of no more than 2% across the samples, indicating a closely matched, if not indistinguishable, morphology or shape of the mAbs. The reported positive value of the net charge, Z, for the mAbs at pH 7.5 is in the same range as those values reported in other studies for IgG1 antibody at pH within 5.0 and 9.0 and low ionic strength. A difference is found between trastuzumab and pertuzumab, explained by the differences in their amino acid sequences (AAS). No appreciable differences have been found between trastuzumab and the two biosimilars, Herzuma and Ontruzant, in this aspect. The thermal stability results, as depicted in Figures S4 and S5, yielded valuable insights into the capacity of the mAbs to uphold their structural integrity and functionality across a spectrum of temperatures. Notably, no discernible disparities in stability were observed among the various antibodies tested, indicating consistent resilience across the antibody samples.

Herceptin and the biosimilars of trastuzumab, namely Ontruzant, and Herzuma, exhibit identical SEC-TD profiles, as demonstrated in Figure 1. Table 1 outlines the main molecular and physical-chemical characteristics of the mAbs and the glycosylated extracellular domain of HER2 (g-

 doi:10.20944/preprints202402.1423.v1

eHER2) utilized in this study. These properties were acquired from the SEC-TD outcomes depicted in Figure 1 and Dynamic Light Scattering (DLS) experiments, conducted at a temperature of T = 309 K (36 °C) as described in the methods section (see also Supplementary Material in which the complete characterization of the mAbs is described). All proteins in this study exhibit the expected molecular and hydrodynamic properties consistent with their AAS. Previous works by our group presented a complete experimental and computational modelling study of the molecular and hydrodynamic details of both HER2 and mAbs, which agree with the results summarized in Table 1 [30,31].

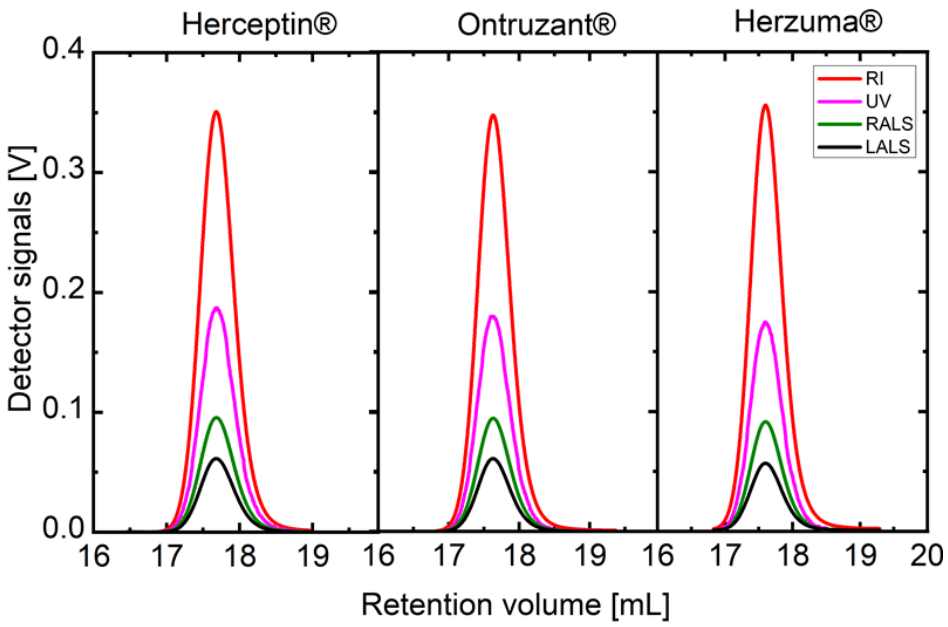

Figure 1. SEC traces for the trastuzumab Herceptin and the biosimilars Ontruzant and Herzuma. Four detectors are indicated: refractive index - RI, ultraviolet - UV, right angle light scattering - RALS and low angle light scattering – LALS, of the biosimilars studied for a concentration of 1.0 mg·mL^{-1} at a temperature of T = 309 K.

Table 1. Molecular and hydrodynamic properties of the mAbs and target HER2; molecular weight (M_w), intrinsic viscosity ([η]), hydrodynamic radius (r_h), and UV coefficient of absorption at 280 nm (dA/dc).

Sample	M_w (kDa)	[η] 10^2 (cm^3·g^{-1}) s.d. ± 0.2	r_h (nm) s.d. ± 0.1	dA/dc (g^{-1}·mL·cm^{-1}) s.d. ± 0.02
Perjeta	147.1 ± 0.8	6.4	5.5	1.33
Herceptin	147.0 ± 1.6	6.5	5.5	1.38
Herzuma	147.9 ± 1.4	6.3	5.5	1.38
Ontruzant	147.7 ± 1.3	6.4	5.5	1.37
g-eHER2	86.3 ± 1.0	6.5	4.4	0.90

Standard deviation values have been obtained from 5 to 10 independent measurements in the same conditions. Theoretical molecular weight values for the mAbs are 145.4 and 145.2 kDa for trastuzumab and pertuzumab, respectively. The experimental value obtained for g-eHER2 includes glycosylation.

We have determined the extinction coefficient, dA/dc, using the UV signal to match protein concentration with that measured from the RI detector. Trastuzumab biosimilars (1.38 ± 0.02 ml·g^{-1}) display a slightly higher value of dA/dc compared to pertuzumab (1.33 ± 0.02 ml·g^{-1}), as expected due to the higher number of aromatic residues in the former. Although both trastuzumab and pertuzumab show a high degree of chemical similarity, there are subtle differences in the amounts of

 doi:10.20944/preprints202402.1423.v1

tyrosine (Tyr), tryptophan (Trp), and phenylalanine (Phe) residues, which can affect the extinction, ε, or absorption coefficient, dA/dc, as measured by UV spectroscopy. The extinction coefficient at 280 nm is unique to each protein and depends on the number of aromatic residues as well as the solvent, temperature, and pH. We used the Protein Calculator Resource (http://protcalc.sourceforge.net/) to compute theoretically dA/dc for the samples under study, utilizing the corresponding AAS. The absorption coefficients in water were estimated in this case using the method of Gill and von Hippel at 280 nm [32]. We tested this procedure using bovine serum albumin, ovoalbumin, and conalbumin protein standards. The experimental values obtained for dA/dc in our SEC-TD system were 0.67, 0.72, and 1.12 $mL \cdot g^{-1} \cdot cm^{-1}$, respectively, which are quite similar to those calculated in silico for these proteins (0.69, 0.73, and 1.11, from the AAS) and reported elsewhere [33]. The values obtained from the calculations for trastuzumab and pertuzumab equal 1.41 and 1.37 $mL \cdot g^{-1}$ at 280 nm, respectively, in close agreement with those measured experimentally.

We tested the ability of the two mAbs trastuzumab and pertuzumab, to bind the HER2 domain in different solutions. We added HER2 to an excess of mAbs in three different cases: 1) to trastuzumab, followed by pertuzumab, 2) to pertuzumab, followed by trastuzumab, and 3) to a 1:1 mixture of both mAbs. In all cases, we maintained the mAbs:HER2 ratio as 3:1. We measured the molecular features of the complexes formed in each case after each step and presented them in Tables 2, 3, and 4. It is important to note that the binding affinity of trastuzumab and pertuzumab to HER2 differs in solution (Figure 2). When HER2 is added to an excess of trastuzumab, it mainly forms a heterodimer (C1, one HER2 domain bound to one mAb Fab, Figure 3A) with a molecular weight of M_w = 235.0 - 240.0 kDa. Additionally, a HER2/mAb/HER2 heterotrimer (C2, two HER2 bounds to the two available mAb Fabs, Figure 3B) is formed with M_w = 310 - 315 kDa. On the other hand, pertuzumab is more likely to form the heterotrimer (C2, Figure 3E) with both Fabs of the mAb bound to two HER2 copies, resulting in a value of $M_w = 310.0 \pm 5.0$ kDa (Figure 2, right panel). The biosimilars Ontruzant and Herzuma showed identical profiles to Herceptin in the binding experiment with HER2 extracellular domain, as they also formed mostly the same complexes in nearly identical proportions, as shown in Figure 2 (left panel). We measured the sizes of the two complexes (C1 and C2) to be different, around 6.2 and 7.3 nm, respectively (see Tables 2 and 3).

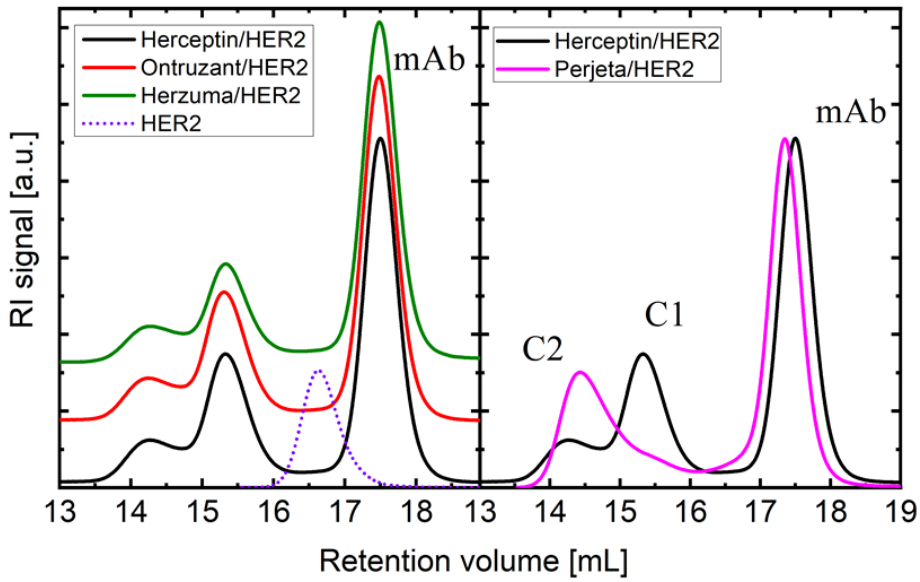

Figure 2. SEC traces of mAb/HER2 complexes. SEC traces (RI signal) of complexes between each trastuzumab biosimilar and HER2 (left), and comparison of trastuzumab/HER2 and pertuzumab/HER2 traces obtained in the same conditions (right).

Preprints.org (www.preprints.org) | NOT PEER-REVIEWED | Posted: 26 February 2024 doi:10.20944/preprints202402.1423.v1

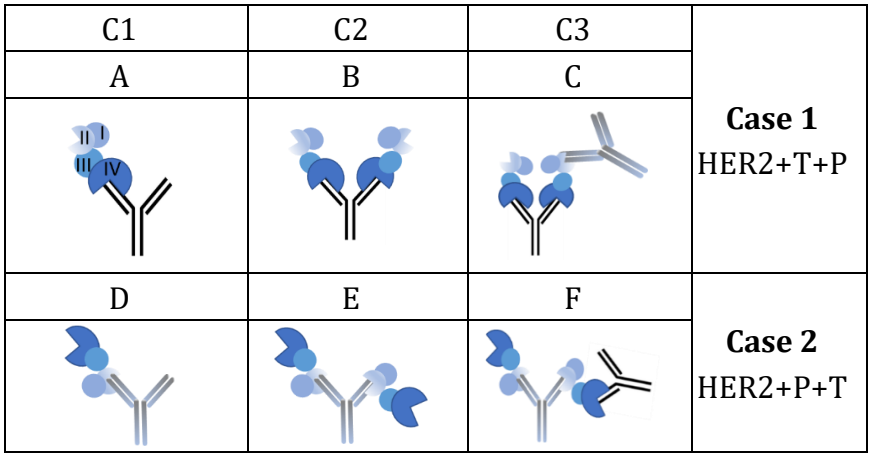

Figure 3. Schematic representation of the different complexes: HER2 extracellular domains (blue), trastuzumab (T, black) and pertuzumab (P, grey). The different HER2 domains are indicated in A.

Table 2. Molecular and hydrodynamic properties of the complexes (case 1); molecular weight, intrinsic viscosity, hydrodynamic radius, and UV coefficient of absorption at 280 nm.

Sample C1/C2	**M_w (kDa)**	**$[\eta]\ 10^2$ ($cm^3 \cdot g^{-1}$) s.d. ± 0.2**	**r_h (nm) s.d. ± 0.1**	**dA/dc ($g^{-1} \cdot mL \cdot cm^{-1}$) s.d. ± 0.02**
HRC/HER2	235.7/310.8	6.7/7.9	6.2/7.1	1.22/1.15
ONT/HER2	237.5/313.6	6.9/7.7	6.2/7.2	1.23/1.14
HZM/HER2	238.2/315.7	6.8/7.8	6.2/7.2	1.22/1.15
C3		**Case 1: TZM/HER2/PZM**		
HRC/HER2/PJT	482.5	8.1	8.5	1.22
ONT/HER2/PJT	483.2	8.2	8.6	1.22

Standard deviations are obtained from the values of M_w by matching concentration in RI and UV detectors. Theoretical M_w is around for C1, C2 and C3 are 234, 320 and 464 kDa, respectively, by assuming the values of M_w in Table 1. HRC, ONT, HZM and PJT stand for Herceptin, Ontruzant, Herzuma and Perjeta, respectively.

Our previous study found that pertuzumab Perjeta has a stronger binding affinity to HER2 than trastuzumab Herceptin. We have explained this difference by analyzing the different interfacial contact (IC) descriptors that contribute to the estimated free energy of binding (ΔG_{bind}) value using a QSAR model [34]. Additionally, we conducted experiments that revealed that the pertuzumab IgG antibody binds to two HER2 proteins, one per Fab fragment, while trastuzumab mainly forms a monovalent complex. We interpreted this finding using a geometrical model that identified steric crowding in the trastuzumab/HER2 heterotrimer compared to the pertuzumab/HER2 heterotrimer. Now, the result observed in Figure 2 demonstrates that the biosimilars Ontruzant and Herzuma behave exactly the same than Herceptin, as the concentration and molecular weight profiles are identically replicated. Small differences in the values for the molecular features (M_w and r_h) and the previous results obtained in our group can be anticipated. We attribute the small changes to the slightly different conditions used [31]. The intrinsic viscosities are in fact slightly lower now, which is a consequence of the higher temperature used in the current set of experiments (T = 307 K) in comparison to that used in reference [31]. Our findings indicate that biosimilars Ontruzant and Herzuma behave likewise to Herceptin, indicating their equivalence in terms of molecular weight and binding affinity to HER2.

In the next step of our study, by adding a second antibody to the solution, larger complexes in all three cases are obtained (around a retention volume of 14 mL). The molecular weight of these complexes is around 480 - 490 kDa, and there are neither differences found in the case of the biosimilars at this point. Figure 4 exemplifies this result, showing the case 2 of addition using pertuzumab (Perjeta) plus trastuzumab, Herceptin, and the biosimilars. The main complex found at

 doi:10.20944/preprints202402.1423.v1

14 mL has a molecular weight that is consistent with the association of two antibodies (trastuzumab and pertuzumab) linked through a HER2 copy, with the other Fab of pertuzumab also linked to a HER2 protein unit (C3, see Figure 3F). Note, that pertuzumab and trastuzumab bind to different HER2 domains (domain II and IV, respectively). The production of the C3 complex with a molecular weight of M_w ~ 480 - 490 kDa was examined in case 1, case 2, and case 3 experiments using Herceptin and the biosimilars Ontruzant and Herzuma. The concentration of the C3 heterocomplex over the total concentration of HER2 added was determined based on RI detector signals, and it was found that the differences in the production of the C3 complex for case 2 experiments (Figure 4) with the different trastuzumab biosimilars were smaller than 1%. The same trend was observed in case 1. Interestingly, in both cases 1 and 2 a very small percentage (around 1 - 3%) of a very high molecular weight complex (M_w ~ 930 kDa) was also detected around a retention volume of 12 mL. This finding again suggests that the biosimilars Ontruzant and Herzuma have a similar capacity as Herceptin to form the C3 complex, indicating that they are biologically equivalent to the reference drug to bind HER2 in presence of pertuzumab and in the conditions under study.

In case 3 experiments, for which HER2 was added to 1:1 mixture of trastuzumab and pertuzumab, a significant increase in the concentration of high-order complexes of M_w = 930 - 940 kDa was measured, appearing at a retention volume of 12 mL. The increase in the production of this complexes with respect to cases 1 and 2, was over one order of magnitude (30%). Figure 5 provides a visual comparison of the results obtained in cases 1, 2, and 3. The signals have been deconvoluted in order to extract the concentration of each species. It is evident that a higher amount of high molecular weight complexes was formed in case 3, and even a small amount of very high molecular weight complexes of around 1,400 kDa was detected, around a retention volume of 10 – 11 mL. For these high-order complexes to form, a bivalent trastuzumab should be involved as a linker (see Figure 6). In that way, the formed complexes of antigens and monoclonal antibodies linked via bivalent binding constitute molecular chains. The formation of such antigen-antibody molecular catenaries was already proposed by Hughes-Jones et al., for the synergistic lysis of red blood cells [35].

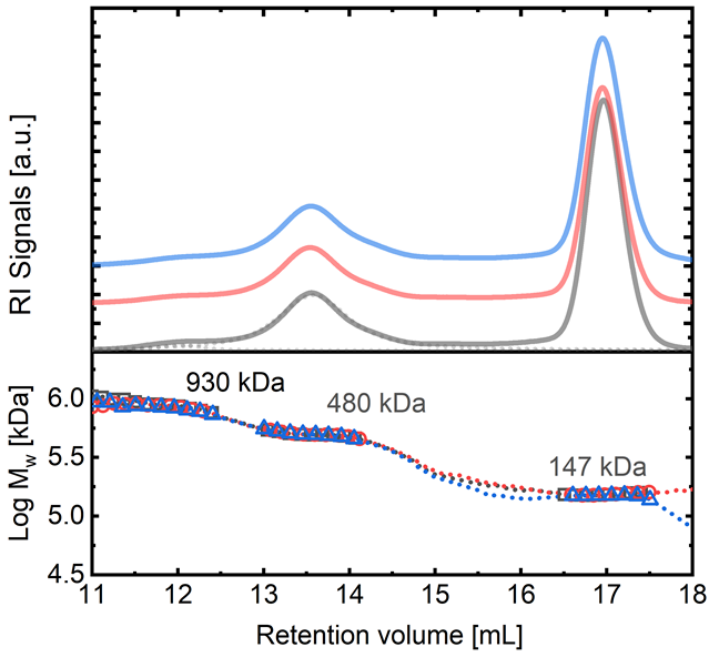

Figure 4. Comparison of the SEC traces obtained for the complexes in case 2. Upper panel: Complete SEC-IR traces of the complexes and free mAb for case 2: black (HRC/HER2/PJT), red (ONT/HER2/PJT) and blue (HZM/HER2/PJT). Curves have been vertically shifted for better visualization. Bottom panel: Measured absolute molecular weight obtained for the complexes.

 doi:10.20944/preprints202402.1423.v1

Table 3. Molecular and hydrodynamic properties of the complexes (case 2); molecular weight, intrinsic viscosity, hydrodynamic radius, and UV coefficient of absorption at 280 nm.

Sample C2	M_w (kDa)	$[\eta]\ 10^2$ ($cm^3 \cdot g^{-1}$) s.d. ± 0.2	r_h (nm) s.d. ± 0.1	dA/dc ($g^{-1} \cdot mL \cdot cm^{-1}$) s.d. ± 0.02
PJT/HER2	310.0	8.0	7.4	1.12
C3		**Case 2: PZM/HER2/TZM**		
PJT/HER2/HRC	484.6	8.1	8.5	1.22
PJT/HER2/ONT	481.8	8.2	8.5	1.23
PJT/HER2/HZM	491.6	8.1	8.6	1.22

Standard deviations are obtained from the values of M_w by matching concentration in RI and UV detectors. Theoretical M_w is around for C1, C2 and C3 are 234, 320 and 464 kDa, respectively, by assuming the values of M_w in Table 1.

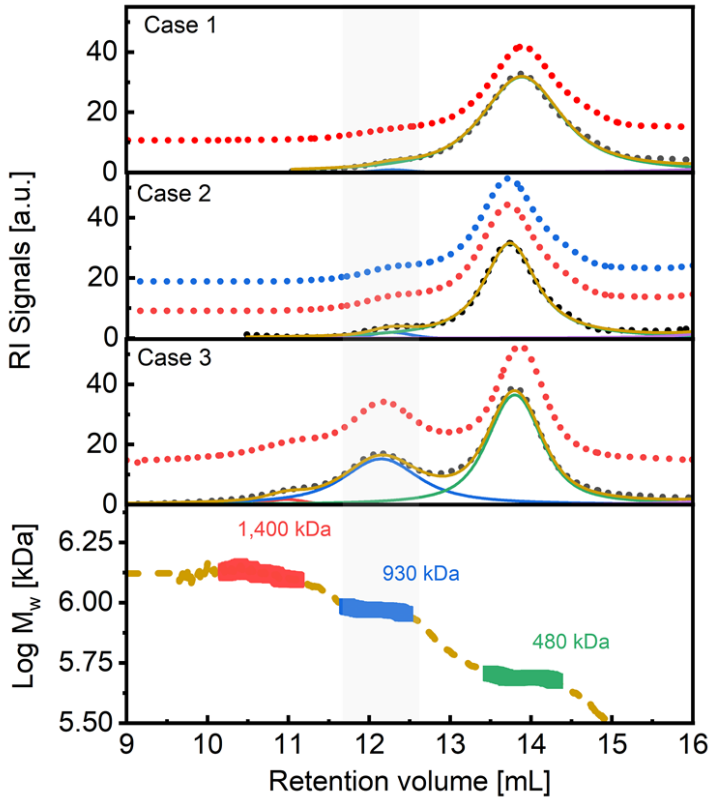

Figure 5. Comparison of the SEC traces obtained for the complexes in case 1, 2 and 3. Upper panels: SEC-IR traces of the complexes formed in the different cases under study. Bottom panel: Measured absolute molecular weight obtained for the complexes. C3 complex appears around 12 mL (grey zone).

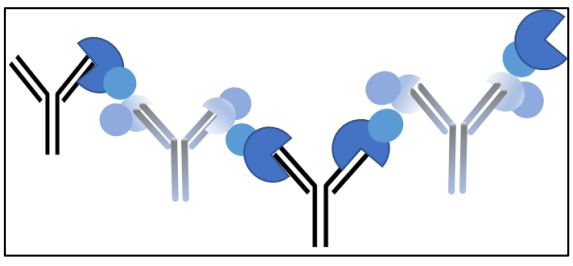

P/T + HER2

 doi:10.20944/preprints202402.1423.v1

Figure 6. High-order complexes (M_w ~ 930 kDa) between the mAbs trastuzumab, pertuzumab and HER2. Pertuzumab, again favors C2 complex in trastuzumab/HER2 interaction acting as linkers. HER2 extracellular domains (blue), trastuzumab (T, black) and pertuzumab (P, grey).

Table 4. Molecular and hydrodynamic properties of the complexes (case 3); molecular weight, intrinsic viscosity, hydrodynamic radius, and UV coefficient of absorption at 280 nm.

Sample	M_w (kDa)	$[\eta]$ 10^2 ($cm^3 \cdot g^{-1}$) s.d. ± 0.2	r_h (nm) s.d. ± 0.1	dA/dc ($g^{-1} \cdot mL \cdot cm^{-1}$) s.d. ± 0.02
C3		**Case 3: TZM/PZM/HER2**		
PJT-HRC/HER2	932.0/489.0	9.8/8.0	9.5/8.7	1.23/1.23
PJT-ONT/HER2	945.0/489.0	n.d./8.2	n.d./8.8	1.25/1.25

Standard deviations are obtained from the values of M_w by matching concentration in RI and UV detectors of the corresponding peaks. Theoretical M_w is around for C1, C2 and C3 are 234, 320 and 464 kDa, respectively, by assuming the values of M_w in Table 1.

The reason for this extremely high avidity of both mAbs together to form these high-order complexes with HER2 is at this moment unknown, but the results suggest an increased availability of trastuzumab Fabs in order to form these complexes, or the appearance of altered intermolecular interactions for binding HER2 to the two mAbs. Further studies are needed to fully understand the mechanisms underlying these observations

3. Materials and Methods

The monoclonal antibodies (mAbs) pertuzumab Perjeta® 450 mg and trastuzumab Herceptin® 150 mg (Roche Pharma AG), trastuzumab biosimilars Ontruzant® 150 mg (SAMSUNG BIOEPIS,), and Herzuma® 150 mg (Celltrion Healthcare) were all obtained from University Hospital Ramón y Cajal (Madrid, Spain) through one of the authors (J.C). The human HER2 (10004-HCCH) extracellular domain was purchased from Sino Biological, Inc. Buffer exchange was performed using centrifugal filter units (Amicon® Ultra-0.5 mL (Merck Millipore). All samples were prepared in buffer 20 mM Tris-Base ULTROL®, 150 mM NaCl, pH 7.5. The initial concentrations of HER2 and mAbs were 0.5 and 1.5 mg·mL-1, respectively.

Dynamic light scattering (DLS) electric field correlations have been obtained for the g-eHER2 and mAbs solutions prepared as indicates above, using the Zetasizer Nano ZS (Malvern Instruments) at T = 309 K, equipped with disposable cuvettes (Malvern Instruments ZEN0040). By the other hand, the electrophoretic mobility (EM) was measured in the Zetasizer Nano ZS apparatus, which uses phase analysis light scattering (PALS). In this application of the technique, a voltage is applied across a pair of electrodes placed at both ends of a disposable capillary cell containing the particle dispersion. Disposable polycarbonate folded capillary cells with gold plated beryllium-copper electrodes (Malvern Instruments DTS1060) were used to perform the measurements. Charged particles are attracted to the oppositely charged electrode, and their velocity was measured and expressed per unit field strength as the EM, μ_e. Measurements were carried out in aliquots of the mAbs stock solutions. The measurements were performed at T = 309 K (36 °C), in samples of c = 5 $mg \cdot mL^{-1}$. Finally, we conducted experiments utilizing DLS to investigate the temperature resistance displayed by the mAbs. By subjecting the samples to varying temperatures, between 293 K (20 °C) to 353 K (80 °C), and monitoring changes in their hydrodynamic size using DLS, we gained insights into the thermal stability of the antibodies. The readers are referred to Supplementary Material for more details about the basic characterization of the mAbs.

The analysis of the binding between mAbs and HER2 receptor and the study of the formed complexes was conducted using SEC-TD. The SEC system used was GPC-TDAmax (Malvern Instruments) equipped with a Superose™ 6 increase 10/300 GL column (Cytiva) was used. The column was equilibrated with a buffer consisting of 20 mM Tris Base Ultrol®, 150 mM NaCl, pH 7.5. Samples of 100 µL were injected into the SEC column and eluted with the buffer at a flow rate of 0.5

 doi:10.20944/preprints202402.1423.v1

mL·min^{-1}. The elution profiles were followed by UV-photo diode array (UV-PDA), differential refractometer (RI), 7° low angle light scattering detector (LALS) and 90° right angle light scattering detector (RALS). The data was acquired and analyzed using OmniSEC software, which determined the absolute molecular weight, M_w, intrinsic viscosity, [η], specific absorption coefficient, dA/dc, and concentration, c, of each sample. The extinction coefficient of each species was obtained by matching the concentration measured by means of the RI detector area to that obtained from the UV detector at 280 nm. The analysis has been performed maintaining the stoichiometry relation of the reaction at 3:1 in all cases. Three experiments were conducted as follows: 1) HER2 was added over trastuzumab. After 30 minutes pertuzumab was added in the same proportion, and the sample was injected after additional 30 minutes. 2) HER2 was added over pertuzumab, and after 30 minutes, trastuzumab was added to the last solution. Conditions and ratio of amounts added were the same as in the first experiment. 3) A solution of trastuzumab and pertuzumab 1:1 was prepared with a concentration of 1 mg·mL^{-1}. Over this mixture, HER2 was added. Bovine serum albumin (Sigma Aldrich) was used as a standard reference protein of known molecular weight, concentration, and refractive index increment (dn/dc = 0.185 mL·g^{-1}). Before each determination, a BSA solution at a concentration of 2 mg·mL^{-1} was used as a standard, allowing for the determination of molecular weight, concentrations, intrinsic viscosity, and extinction coefficients of the mAbs, HER2 protein, and the complexes.

4. Conclusions

The results presented in this study confirm the similar efficacy of trastuzumab biosimilars when used in combination with pertuzumab. Furthermore, the results settle that the coformulation of mixtures of therapeutic mAbs targeting multiple epitopes represents an appealing strategy to increase their efficacy [36,37] and approach the goal of mimicking the natural polyclonal humoral immune response [38]. Although there are few systematic studies on this approach, reports on mAb mixtures for the treatment of various diseases are emerging [38–40]. At this respect, it is important to understand the potential interactions between mAbs and the effects of variables such as pH, concentration, temperature, and ionic strength [41]. In the specific case of the pertuzumab/trastuzumab mixtures, it should be noted that a fixed-dose combination of pertuzumab and trastuzumab for subcutaneous injection (PHESGO™, F. Hoffmann-La Roche Ltd.) has recently been approved by the U.S. Food and Drug Administration (FDA) and the European Medicines Agency. These findings have important implications for the development of this type therapeutic mAb combinations [42].

Supplementary Materials: The supporting material file can be downloaded at the website of this paper posted on Preprints.org.

Author Contributions: Conceptualization, J.F.V., J.R. and J.C.; supervision, J.F.V. and J.C.; validation, J.F.V., J.R., and J.C.; formal analysis, J.F.V., J.R. and V.L.C.; writing - original draft, J.F.V. and V.S.E.; writing - review & editing, J.F.V., J.R., V.L.C., J.C.; project administration, J.F.V.; funding acquisition – J.F.V., J.R., J.C.; resources: J.C., L.C.E., J.P.G., M.G:, L.G., P.C., C.S., P.G. and C.O.; investigation and methodolody, E.F.M, VSE, L.C.E., J.P.G., M.G:, L.G., P.C., C.S., P.G. and C.O.; data curation, E.F.M. and VSE. All authors have read and agreed to the published version of the manuscript.

Funding: This research work was funded by the Fundación FERO and Fundación "Contigo contra el cancer de la mujer" (With you against women cancer). J.R. and J.F.V acknowledge support by CSIC under the Grants PIE202050E017 and PIE202350E113.

Data Availability Statement: The data presented in this study are available on request from the corresponding author.

Conflicts of Interest: The authors declare that they have no known competing financial interests or personal relationships that could have appeared to influence the work reported in this paper.

References

1. Swain, S.M.; Shastry, M.; Hamilton, E. Targeting HER2-Positive Breast Cancer: Advances and Future Directions. Nat Rev Drug Discov 2023, 22, 101–126, doi:10.1038/s41573-022-00579-0.

2. Giordano, S.H.; Temin, S.; Davidson, N.E. Systemic Therapy for Patients with Advanced Human Epidermal Growth Factor Receptor 2-Positive Breast Cancer: ASCO Clinical Practice Guideline Update Summary. J Oncol Pract 2018, 14, 501–504, doi:10.1200/JOP.18.00290.
3. Hudis, C.A. Trastuzumab - Mechanism of Action and Use in Clinical Practice. New England Journal of Medicine 2007, 357, 39–51, doi:10.1056/NEJMra043186.
4. De Mattos-Arruda, L.; Cortes, J. Use of Pertuzumab for the Treatment of HER2-Positive Metastatic Breast Cancer. Adv Ther 2013, 30, 645–658, doi:10.1007/s12325-013-0043-2.
5. Von Minckwitz, G.; Procter, M.; De Azambuja, E.; Zardavas, D.; Benyunes, M.; Viale, G.; Suter, T.; Arahmani, A.; Rouchet, N.; Clark, E.; et al. Adjuvant Pertuzumab and Trastuzumab in Early Her2-Positive Breast Cancer. New England Journal of Medicine 2017, 377, 122–131, doi:10.1056/NEJMoa1703643.
6. Jagosky, M.; Tan, A.R. Combination of Pertuzumab and Trastuzumab in the Treatment of Her2-Positive Early Breast Cancer: A Review of the Emerging Clinical Data. Breast Cancer: Targets and Therapy 2021, 13, 393–407, doi:10.2147/BCTT.S176514.
7. Liu, X.; Fang, Y.; Li, Y.; Li, Y.; Qi, L.; Wang, X. Pertuzumab Combined with Trastuzumab Compared to Trastuzumab in the Treatment of HER2-Positive Breast Cancer: A Systematic Review and Meta-Analysis of Randomized Controlled Trials. Front Oncol 2022, 12, 894861, doi:10.3389/fonc.2022.894861.
8. Baselga, J.; Cortés, J.; Kim, S.-B.; Im, S.-A.; Hegg, R.; Im, Y.-H.; Roman, L.; Pedrini, J.L.; Pienkowski, T.; Knott, A.; et al. Pertuzumab plus Trastuzumab plus Docetaxel for Metastatic Breast Cancer. New England Journal of Medicine 2012, 366, 109–119, doi:10.1056/NEJMoa1113216.
9. Swain, S.M.; Baselga, J.; Kim, S.-B.; Ro, J.; Semiglazov, V.; Campone, M.; Ciruelos, E.; Ferrero, J.-M.; Schneeweiss, A.; Heeson, S.; et al. Pertuzumab, Trastuzumab, and Docetaxel in HER2-Positive Metastatic Breast Cancer. New England Journal of Medicine 2015, 372, 724–734, doi:10.1056/NEJMoa1413513.
10. Krop, I.E.; Modi, S.; LoRusso, P.M.; Pegram, M.; Guardino, E.; Althaus, B.; Lu, D.; Strasak, A.; Elias, A. Phase 1b/2a Study of Trastuzumab Emtansine (T-DM1), Paclitaxel, and Pertuzumab in HER2-Positive Metastatic Breast Cancer. Breast Cancer Research 2016, 18, 34, doi:10.1186/s13058-016-0691-7.
11. Miller, K.D.; Diéras, V.; Harbeck, N.; Andre, F.; Mahtani, R.L.; Gianni, L.; Albain, K.S.; Crivellari, D.; Fang, L.; Michelson, G.; et al. Phase IIa Trial of Trastuzumab Emtansine with Pertuzumab for Patients with Human Epidermal Growth Factor Receptor 2-Positive, Locally Advanced, or Metastatic Breast Cancer. Journal of Clinical Oncology 2014, 32, 1437–1444, doi:10.1200/JCO.2013.52.6590.
12. Urruticoechea, A.; Rizwanullah, M.; Im, S.-A.; Sánchez Ruiz, A.C.; Láng, I.; Tomasello, G.; Douthwaite, H.; Crnjevic, T.B.; Heeson, S.; Eng-Wong, J.; et al. Randomized Phase III Trial of Trastuzumab plus Capecitabine with or without Pertuzumab in Patients with Human Epidermal Growth Factor Receptor 2-Positive Metastatic Breast Cancer Who Experienced Disease Progression during or after Trastuzumab-Based Therapy. Journal of Clinical Oncology 2017, 35, 3030–3038, doi:10.1200/JCO.2016.70.6267.
13. Rimawi, M.; Ferrero, J.-M.; De La Haba-Rodriguez, J.; Poole, C.; De Placido, S.; Osborne, C.K.; Hegg, R.; Easton, V.; Wohlfarth, C.; Arpino, G. First-Line Trastuzumab plus an Aromatase Inhibitor, with or without Pertuzumab, in Human Epidermal Growth Factor Receptor 2-Positive and Hormone Receptor-Positive Metastatic or Locally Advanced Breast Cancer (PERTAIN): A Randomized, Open-Label Phase II Trial. Journal of Clinical Oncology 2018, 36, 2826–2835, doi:10.1200/JCO.2017.76.7863.
14. Perez, E.A.; Barrios, C.; Eiermann, W.; Toi, M.; Im, Y.-H.; Conte, P.; Martin, M.; Pienkowski, T.; Pivot, X.B.; Burris, H.A.; et al. Trastuzumab Emtansine with or without Pertuzumab versus Trastuzumab with Taxane for Human Epidermal Growth Factor Receptor 2–Positive Advanced Breast Cancer: Final Results from MARIANNE. Cancer 2019, 125, 3974–3984, doi:10.1002/cncr.32392.
15. Patel, T.A.; Ensor, J.E.; Creamer, S.L.; Boone, T.; Rodriguez, A.A.; Niravath, P.A.; Darcourt, J.G.; Meisel, J.L.; Li, X.; Zhao, J.; et al. A Randomized, Controlled Phase II Trial of Neoadjuvant Ado-Trastuzumab Emtansine, Lapatinib, and Nab-Paclitaxel versus Trastuzumab, Pertuzumab, and Paclitaxel in HER2-Positive Breast Cancer (TEAL Study). Breast Cancer Research 2019, 21, 100, doi:10.1186/s13058-019-1186-0.
16. Swain, S.M.; Miles, D.; Kim, S.-B.; Im, Y.-H.; Im, S.-A.; Semiglazov, V.; Ciruelos, E.; Schneeweiss, A.; Loi, S.; Monturus, E.; et al. Pertuzumab, Trastuzumab, and Docetaxel for HER2-Positive Metastatic Breast Cancer (CLEOPATRA): End-of-Study Results from a Double-Blind, Randomised, Placebo-Controlled, Phase 3 Study. Lancet Oncol 2020, 21, 519–530, doi:10.1016/S1470-2045(19)30863-0.
17. Xu, B.; Li, W.; Zhang, Q.; Li, Q.; Wang, X.; Li, H.; Sun, T.; Yin, Y.; Zheng, H.; Feng, J.; et al. Pertuzumab, Trastuzumab, and Docetaxel for Chinese Patients with Previously Untreated HER2-Positive Locally Recurrent or Metastatic Breast Cancer (PUFFIN): Final Analysis of a Phase III, Randomized, Double-Blind, Placebo-Controlled Study. Breast Cancer Res Treat 2023, 197, 503–513, doi:10.1007/s10549-022-06775-1.
18. Phillips, G.D.L.; Fields, C.T.; Li, G.; Dowbenko, D.; Schaefer, G.; Miller, K.; Andre, F.; Burris III, H.A.; Albain, K.S.; Harbeck, N.; et al. Dual Targeting of HER2-Positive Cancer with Trastuzumab Emtansine and

Pertuzumab: Critical Role for Neuregulin Blockade in Antitumor Response to Combination Therapy. Clinical Cancer Research 2014, 20, 456–468, doi:10.1158/1078-0432.CCR-13-0358.
19. Wang, C.; Chen, J.; Xu, X.; Hu, X.; Kong, D.; Liang, G.; Wang, X. Dual HER2 Blockade in Neoadjuvant Treatment of HER2+ Breast Cancer: A Meta-Analysis and Review. Technol Cancer Res Treat 2020, 19, 1–10, doi:10.1177/1533033820960721.
20. Triantafyllidi, E.; Triantafillidis, J.K. Systematic Review on the Use of Biosimilars of Trastuzumab in HER2+ Breast Cancer. Biomedicines 2022, 10, 2045, doi:10.3390/biomedicines10082045.
21. Waller, C.F.; Möbius, J.; Fuentes-Alburo, A. Intravenous and Subcutaneous Formulations of Trastuzumab, and Trastuzumab Biosimilars: Implications for Clinical Practice. Br J Cancer 2021, 124, 1346–1352, doi:10.1038/s41416-020-01255-z.
22. Janjigian, Y.Y.; Bissig, M.; Curigliano, G.; Coppola, J.; Latymer, M. Talking to Patients about Biosimilars. Future Oncology 2018, 14, 2403–2414, doi:10.2217/fon-2018-0044.
23. Miller, E.M.; Schwartzberg, L.S. Biosimilars for Breast Cancer: A Review of HER2-Targeted Antibodies in the United States. Ther Adv Med Oncol 2019, 11, 1–9, doi:10.1177/1758835919887044.
24. Oda, M.; Uchiyama, S.; Noda, M.; Nishi, Y.; Koga, M.; Mayanagi, K.; Robinson, C. V; Fukui, K.; Kobayashi, Y.; Morikawa, K.; et al. Effects of Antibody Affinity and Antigen Valence on Molecular Forms of Immune Complexes. Mol Immunol 2009, 47, 357–364, doi:https://doi.org/10.1016/j.molimm.2009.09.009.
25. Wen, J.; Arakawa, T.; Wypych, J.; Langley, K.E.; Schwartz, M.G.; Philo, J.S. Chromatographic Determination of Extinction Coefficients of Non-Glycosylated Proteins Using Refractive Index (RI) and UV Absorbance (UV) Detectors: Applications for Studying Protein Interactions by Size Exclusion Chromatography with Light-Scattering, UV, and RI Detectors. Techniques in Protein Chemistry 1997, 8, 113–119, doi:10.1016/S1080-8914(97)80014-2.
26. Arakawa, T.; Wen, J. Size-Exclusion Chromatography with on-Line Light Scattering. Current protocols in protein science 2001, Chapter 20, 20.6.1-20.6.1.
27. Mayer, C.L.; Snyder, W.K.; Swietlicka, M.A.; Vanschoiack, A.D.; Austin, C.R.; McFarland, B.J. Size-Exclusion Chromatography Can Identify Faster-Associating Protein Complexes and Evaluate Design Strategies. BMC Res Notes 2009, 2, 135, doi:10.1186/1756-0500-2-135.
28. Bai, Y. Detecting Protein-Protein Interactions by Gel Filtration Chromatography. In Protein-Protein Interactions: Methods and Applications: Second Edition; 2015; pp. 223–232.
29. Goyon, A.; Fekete, S.; Beck, A.; Veuthey, J.-L.; Guillarme, D. Unraveling the Mysteries of Modern Size Exclusion Chromatography - the Way to Achieve Confident Characterization of Therapeutic Proteins. J Chromatogr B Analyt Technol Biomed Life Sci 2018, 1092, 368–378, doi:10.1016/j.jchromb.2018.06.029.
30. Vega, J.F.; Ramos, J.; Cruz, V.L.; Vicente-Alique, E.; Sánchez-Sánchez, E.; Sánchez-Fernández, A.; Wang, Y.; Hu, P.; Cortés, J.; Martínez-Salazar, J. Molecular and Hydrodynamic Properties of Human Epidermal Growth Factor Receptor HER2 Extracellular Domain and Its Homodimer: Experiments and Multi-Scale Simulations. Biochim Biophys Acta Gen Subj 2017, 1861, 2406–2416, doi:10.1016/j.bbagen.2017.06.012.
31. Ramos, J.; Vega, J.F.; Cruz, V.; Sanchez-Sanchez, E.; Cortes, J.; Martinez-Salazar, J. Hydrodynamic and Electrophoretic Properties of Trastuzumab/HER2 Extracellular Domain Complexes as Revealed by Experimental Techniques and Computational Simulations. Int J Mol Sci 2019, 20, 1076, doi:10.3390/ijms20051076.
32. Gill, S.C.; von Hippel, P.H. Calculation of Protein Extinction Coefficients from Amino Acid Sequence Data. Anal Biochem 1989, 182, 319–326, doi:10.1016/0003-2697(89)90602-7.
33. Pace, C.N.; Vajdos, F.; Fee, L.; Grimsley, G.; Gray, T. How to Measure and Predict the Molar Absorption Coefficient of a Protein. Protein Science 1995, 4, 2411–2423, doi:10.1002/pro.5560041120.
34. Cruz, V.L.; Souza-Egipsy, V.; Gion, M.; Pérez-García, J.; Cortes, J.; Ramos, J.; Vega, J.F. Binding Affinity of Trastuzumab and Pertuzumab Monoclonal Antibodies to Extracellular HER2 Domain. Int J Mol Sci 2023, 24, doi:10.3390/ijms241512031.
35. Hughes-Jones, N.C.; Gorick, B.D.; Howard, J.C. The Mechanism of Synergistic Complement-Mediated Lysis of Rat Red Cells by Monoclonal IgG Antibodies. Eur J Immunol 1983, 13, 635–641, doi:https://doi.org/10.1002/eji.1830130806.
36. Robak, T. The Emerging Therapeutic Role of Antibody Mixtures. Expert Opin Biol Ther 2013, 13, 953–958, doi:10.1517/14712598.2013.799133.
37. Raju, T.S.; Strohl, W.R. Potential Therapeutic Roles for Antibody Mixtures. Expert Opin Biol Ther 2013, 13, 1347–1352, doi:10.1517/14712598.2013.822065.
38. Larbouret, C.; Gros, L.; Pèlegrin, A.; Chardès, T. Improving Biologics' Effectiveness in Clinical Oncology: From the Combination of Two Monoclonal Antibodies to Oligoclonal Antibody Mixtures. Cancers (Basel) 2021, 13, 4620, doi:10.3390/cancers13184620.

39. Skartved, N.J.Ø.; Jacobsen, H.J.; Pedersen, M.W.; Jensen, P.F.; Sen, J.W.; Jørgensen, T.K.; Hey, A.; Kragh, M. Preclinical Pharmacokinetics and Safety of Sym004: A Synergistic Antibody Mixture Directed against Epidermal Growth Factor Receptor. Clinical Cancer Research 2011, 17, 5962–5972, doi:10.1158/1078-0432.CCR-11-1209.
40. Meng, Q.; Garcia-Rodriguez, C.; Manzanarez, G.; Silberg, M.A.; Conrad, F.; Bettencourt, J.; Pan, X.; Breece, T.; To, R.; Li, M.; et al. Engineered Domain-Based Assays to Identify Individual Antibodies in Oligoclonal Combinations Targeting the Same Protein. Anal Biochem 2012, 430, 141–150, doi:10.1016/j.ab.2012.08.005.
41. Singh, P.; Roche, A.; Van Der Walle, C.F.; Uddin, S.; Du, J.; Warwicker, J.; Pluen, A.; Curtis, R. Determination of Protein-Protein Interactions in a Mixture of Two Monoclonal Antibodies. Mol Pharm 2019, 16, 4775–4786, doi:10.1021/acs.molpharmaceut.9b00430.
42. Wang, B.; Deng, R.; Hennig, S.; Badovinac Crnjevic, T.; Kaewphluk, M.; Kågedal, M.; Quartino, A.L.; Girish, S.; Li, C.; Kirschbrown, W.P. Population Pharmacokinetic and Exploratory Exposure–Response Analysis of the Fixed-Dose Combination of Pertuzumab and Trastuzumab for Subcutaneous Injection in Patients with HER2-Positive Early Breast Cancer in the FeDeriCa Study. Cancer Chemother Pharmacol 2021, 88, 499–512, doi:10.1007/s00280-021-04296-0.
43. Yadav, S.; Liu, J.; Shire, S.J.; Kalonia, D.S. Specific interactions in high concentration antibody solutions resulting in high viscosity. J Pharm Sci 2010, 99(3), 1152-68, doi: https://doi.org/10.1002/jps.21898
44. Saito, S.; Hasegawa, J.; Kobayashi, N.; Kishi, N.; Uchiyama, S.; Fukui, K. Behavior of Monoclonal Antibodies: Relation Between the Second Virial Coefficient (B2) at Low Concentrations and Aggregation Propensity and Viscosity at High Concentrations. Pharmaceutical Research 2012, 29, 397–410, doi:https://doi.org/10.1007/s11095-011-0563-x
45. Barnett, G. V.; Qi, W.; Amin, S.; Lewis, E.N.; Razinkov, V.I.; Kerwin, B.A.; Liu, Y.; Roberts, C.J. Structural Changes and Aggregation Mechanisms for AntiStreptavidin IgG1 at Elevated Concentration. J Phys Chem B 2015, 119, 15150−15163, doi:https://doi.org/10.1021/acs.jpcb.5b08748
46. Jaccoulet, E.; Boccard, J.; Taverna, M.; Azevedos, A.S.; Rudaz, S.; Smadja, C. High-throughput identification of monoclonal antibodies after compounding by UV spectroscopy coupled to chemometrics analysis. Anal Bioanal Chem 2016, 408, 5915–5924, doi:https://doi.org/10.1007/s00216-016-9708-4
47. Vermeer A. W. P.; Norde, W. The Thermal Stability of Immunoglobulin: Unfolding and Aggregation of a Multi-Domain Protein Biophys J 2000, 78, 394–404, doi:https://doi.org/10.1016%2FS0006-3495(00)76602-1
48. Le Basle, Y.; Chenell, P.; Tokhadze N.; Astier, A.; Sautou, V. Physicochemical Stability of Monoclonal Antibodies: A Review. J Pharm Sci 2020, 109, 169-190, doi:https://doi.org/10.1016/j.xphs.2019.08.009
49. Lehermayr, C.; Mahler, H.-C.; Mäder, K.; Fischer, S. Assessment of Net Charge and Protein–Protein Interactions of Different Monoclonal Antibodies. J Pharm Sci 2011, 100, 2551–2562, doi: https://doi.org/10.1002/jps.22506
50. Roberts, D.; Keeling, R.; Tracka, M.; van der Walle, C.F.; Uddin, S.; Warwicker, J.; Curtis, R. The Role of Electrostatics in Protein–Protein Interactions of a Monoclonal Antibody. Mol Pharm 2014, 11, 2475–2489, doi: https://doi.org/10.1021/mp5002334
51. Kiraga, J.; Mackiewicz, P.; Mackiewicz, D.; Kowalczuk, M.; Biecek, P.; Polak, N.; Smolarczyk, K.; Dudek, M.R.; Cebrat, S. The relationships between the isoelectric point and: length of proteins, taxonomy and ecology of organisms. BMC Genomics 2007, 8, 163, doi: https://doi.org/10.1186/1471-2164-8-163
52. Knight, C.G.; Kassen, R.; Hebestreit, H.; Rainey, P.B. Global analysis of predicted proteomes: functional adaptation of physical properties. Proc Natl Acad Sci USA 2004, 101, 8390–8395, doi: https://doi.org/10.1073/pnas.0307270101
53. Wang, M.; Zhu, D.; Zhu, J.; Nussinov, R.; Ma, B. Local and Global Anatomy of Antibody-Protein Antigen Recognition. J Mol Recognit 2018, 31(5), e2693, doi: https://doi.org/10.1002/jmr.2693